Transparent Boundary Conditions for Wave Propagation on Unbounded Domains

Dorin-Cezar Ionescu[1] and Heiner Igel[2]

[1] Queensland University Advanced Centre for Earthquake Studies (QUAKES)
The University of Queensland, Brisbane, QLD 4072, Australia
[2] Institut für Angewandte Geophysik, Ludwig-Maximilians-Universität München
Theresienstr. 41, 80333 München, Germany

Abstract. The numerical solution of the time dependent wave equation in an unbounded domain generally leads to a truncation of this domain, which requires the introduction of an artificial boundary with associated boundary conditions. Such exact nonreflecting conditions ensure the equivalence between the solution of the original problem in the unbounded region and the solution inside the artificial boundary. We consider absorbing boundary condition techniques for the wave equation and their numerical implementation in a finite difference approach. In particular, exact conditions that annihilate wave harmonics on a spherical artificial boundary up to a given order are discussed and subsequently applied for the practical simulation of acoustic wave propagation. The analysis is complemented by numerical examples illustrating the accuracy of transparent boundary conditions.

1 Introduction

Modern trends in the development of numerical methods lead to higher and higher requirements for the computational accuracy. Solving numerically the wave equation for modelling wave propagation on unbounded domains with complex geometry requires a truncation, to fit the infinite region on a finite computer. Minimizing the amount of spurious reflections requires in many cases the introduction of an artificial boundary and of associated absorbing boundary conditions. The critical importance of these techniques becomes particularly evident when one considers that the gains made in the computational domain by using sophisticated high order and/or adaptive numerical approaches may vanish to a large extent as result of violating the boundary conditions at the artificial boundary.

Despite the computational speed of finite difference schemes and the robustness of finite elements in handling complex geometries the resulting numerical error consists of two independent contributions: the discretization error of the numerical method used and the spurious reflection generated at the artificial boundary. This spurious contribution travels back and substantially degrades the accuracy of the solution everywhere in the computational domain. Unless

both error components are reduced systematically, the numerical solution does not converge to the solution of the original problem in the infinite region.

There are several techniques for approximately handling with boundary conditions at the external boundary of a finite computational domain that is obtained from the original unbounded domain by means of truncation. While a first group of boundary conditions is given by local differential operators [2], [3], including boundary conditions that perfectly annihilate impinging waves at a finite number of *selected* angles of incidence [4], a different approximate approach is based on absorbing layers [5]. Exact nonreflecting boundary conditions for the scalar, Maxwell and elasto-dynamic equations were derived by Grote and Keller [6], [7], using an approach based on integral transforms. There are cases, where some of the difficulties with boundary conditions may be avoided partially by using a momentum space approach [8], [9]. In contrast to grid methods in coordinate space where continuum waves spread over the entire space, in momentum space the waves are confined to a small finite volume and the dynamics stays localized around the origin at all times.

In the present work we discuss absorbing boundary condition techniques for the scalar wave equation. In contrast to [6] were an integral equation is used, our approach is based on a recurrence relation that provides a straightforward derivation of the boundary condition. In addition, we present the numerical implementation using a finite difference method. In Sec. 2, we illustrate the fundamental ideas underlying the derivation of exact absorbing boundary conditions for the one-dimensional wave equation and present the extension to higher dimensions. In Sec. 3 we present and discuss numerical examples based on finite differences. The conclusions of the present study are given in Sec. 4.

2 Theoretical Approach

2.1 The One-Dimensional Wave Equation

We consider the one-dimensional wave equation describing the propagation of perturbations along the positive real axis ($x \geq 0, t \geq 0$) with velocity $c = 1$ that are induced by an applied forcing term $f(x,t)$

$$\left(\partial_t^2 \;-\; \partial_x^2\right) \Phi(x,t) \;\;=\;\; f(x,t) \;\;, \tag{1}$$

where $\Phi(x,t)$ represents the displacement of an infinitely long string and $\partial_t = \partial/\partial t$. Requiring $\Phi(0,t) = 0$ for the state at rest, $\Phi(x,t)$ describes the position of a string that is fixed at one end. We define the initial conditions by the string position and velocity at $t = 0$ by $\Phi(x,0) = U_0$ and $\partial_t \Phi(x,t) \mid_{t=0} = V_0$.

The local character of the problem is defined by assuming $f(x,t) = 0$ for $x \geq L$, $\forall\, t \geq 0$. Thus, the positive x-axis separates into two distinctly different regions: the bounded (interior) domain $x \leq L$, and the unbounded (exterior) region $x \geq L$ where the forcing term f vanishes. The two regions are separated by the artificial boundary at $x = L$.

For finding the exact absorbing boundary condition at $x = L$ it is useful to separate outgoing from incoming waves by defining

$$\begin{aligned} v &= \partial_t \Phi + \partial_x \Phi \ , \\ w &= \partial_t \Phi - \partial_x \Phi \ . \end{aligned} \tag{2}$$

Since $\Phi(x,t)$ is a solution of Eq. (1) for $x \geq L$, i.e. $(\partial_t^2 - \partial_x^2)\Phi = 0$, one has with (2) in the exterior region

$$\begin{aligned} 0 &= (\partial_t - \partial_x)\left[(\partial_t + \partial_x)\Phi\right] = (\partial_t - \partial_x)v \ , \\ 0 &= (\partial_t + \partial_x)\left[(\partial_t - \partial_x)\Phi\right] = (\partial_t + \partial_x)w \ . \end{aligned} \tag{3}$$

or

$$\begin{pmatrix} v \\ w \end{pmatrix} + \begin{pmatrix} -1 & 0 \\ 0 & 1 \end{pmatrix} \partial_x \begin{pmatrix} v \\ w \end{pmatrix} = 0 \ , \tag{4}$$

This first order equation has the general solution

$$\begin{aligned} v(x,t) &= \psi(x+t) \ , \\ w(x,t) &= \varphi(x-t) \ , \end{aligned} \tag{5}$$

where ψ and φ are arbitrary functions that are determined by initial and boundary conditions. It follows for incoming (v)and outgoing (w) waves, respectively,

$$\begin{aligned} v(x,t) &= \text{const., for } x + t = \text{const.} \quad \text{(incoming)} \\ w(x,t) &= \text{const., for } x - t = \text{const} \quad \text{(outgoing)} \ . \end{aligned} \tag{6}$$

Since there are no incoming waves in the exterior region, $x \geq L$, it follows $v(L,t) = 0$, for $t \geq 0$. By combining eq. (2) and the last expression, the exact absorbing boundary condition for the displacement $\Phi(x,t)$ may be written as

$$(\partial_t - \partial_x)\,\Phi(x,t)\,|_{x=L} = 0 \ . \tag{7}$$

This expression which is local in time guarantees that the artificial boundary at $x = L$ is perfectly transparent to both incoming and outgoing waves as they leave the interior region without any spurious reflection. We emphasize that the derivation of the exact absorbing boundary condition (7) depends solely on properties in the exterior domain, $x \geq L$.

2.2 Transparent Boundary Conditions in Higher Dimensions

The derivation of exact absorbing boundary conditions in higher dimensions is considerably more challenging as compared to the one dimensional case discussed previously. Distinctly different from the one-dimensional case where waves can propagate in two directions only, in two and more dimensions waves propagate in infinitely many directions.

In the following we consider wave propagation in an unbounded region $\mathbb{R}^3$ and surround the computational region $\tilde{\Omega}$ containing the forcing term $f(\mathbf{r},t)$ by an artificial boundary S that is assumed to be a sphere with radius R. In the exterior domain $\mathbb{R}^3 \setminus \tilde{\Omega}$, $f(\mathbf{r},t) = 0$ and the wave function $\psi(\mathbf{r},t)$ satisfies the homogeneous wave equation with constant propagation velocity $c > 0$, i.e.

$$\left(\frac{1}{c^2}\,\partial_t^2 \;-\; \Delta\right)\psi(\mathbf{r},t) \;=\; 0 \;\text{ in }\; \mathbb{R}\setminus\tilde{\Omega} \;\;, \tag{8}$$

with initial conditions $\psi(\mathbf{r},0) = 0$ and $\dot{\psi}(\mathbf{r},0) = 0$ for $|\mathbf{r}| \geq R$. Since the waves generated inside $\tilde{\Omega}$ propagate into the exterior unbounded region, the wave function $\psi(\mathbf{r},t) \neq 0$ with increasing time. It is useful to insert a multipole decomposition of the solution in spherical coordinates r, ϑ, φ

$$\psi(\mathbf{r},t) \;=\; \sum_{l=0}^{\infty}\sum_{m=-l}^{l} \psi_{l,m}(r,t)\, Y_{l,m}(\vartheta,\varphi) \;\;, \tag{9}$$

where the spherical harmonics

$$Y_{l,m}(\vartheta,\varphi)\psi(\mathbf{r},t) \;=\; \sqrt{\frac{(2\,l\;+\;1)\,(l\;-\;|m|)!}{4\pi\,(l\;+\;|m|)!}}\; P_l^{|m|}(\cos\vartheta)\; e^{im\varphi} \;\;, \tag{10}$$

are orthonormal and the functions $P_l^{|m|}$ are Legendre polynomials. Using the orthonormality properties of the $Y_{l,m}$ the radial time-dependent functions $\psi_{l,m}(r,t)$ may be written as

$$\psi_{l,m}(r,t) \;=\; \int_0^{\pi} d\vartheta\, \sin\vartheta \int_0^{2\pi} d\varphi\; Y_{l,m}^*(\vartheta,\varphi)\; \psi(r,\vartheta,\varphi,t) \;\;. \tag{11}$$

We note that in two dimensions, expansion (10) is ϑ-independent, i.e. one has $\psi(\mathbf{r},t) = \sum_{m=-\infty}^{\infty} \psi_m(r,t)\exp(im\varphi)$. By inserting expression (11) in eq. (2) one obtains the radial equation

$$\left[\frac{1}{c^2}\,\partial_t^2 \;-\; \partial_r^2 \;-\; \frac{2}{r}\,\partial_r \;+\; \frac{l(l+1)}{r^2}\right]\psi_{l,m}(r,t) \;=\; 0 \;\;, \tag{12}$$

with the initial conditions $\psi_{l,m}(r,0) = 0$ and $\dot{\psi}_{l,m}(r,0) = 0$ in the domain $r \geq R$. Noticing that the differential operator contained in the square brackets which we denote by R_l, satisfies a remarkable commutation-like relation [10], [11]

$$R_l\left(\partial_r \;-\; \frac{l-1}{r}\right)\psi_{l,m}(r,t) \;=\; \left(\partial_r \;-\; \frac{l-1}{r}\right) R_{l-1}\,\psi_{l-1,m}(r,t) \;=\; 0\,, \tag{13}$$

one obtains the following recurrence relation for the radial functions

$$\psi_{l,m}(r,t) \;=\; [\partial_r \;-\; (l\,-\,1)/r)]\;\psi_{l-1,m}(r,t)\;\;. \tag{14}$$

Recursive use of the last relation yields

$$\psi_l \;=\; \left(\partial_r \;-\; \frac{l-1}{r}\right)\left(\partial_r \;-\; \frac{l-2}{r}\right)\psi_{l-2} \;=\; \ldots \;=\; \prod_{i=1}^{l}\left(\partial_r \;-\; \frac{i-1}{r}\right)\psi_0 \tag{15}$$

where we substituted $\psi_l = \psi_{l,m}$. Since ψ_0 is a solution of the radial equation (12) with $l = 0$, we find that the modified radial function $\Phi(r,t) = r\psi_0$ satisfies a simple one-dimensional wave equation, i.e.

$$\left(\frac{1}{c^2}\,\partial_t^2 \;\;-\;\;\partial_r^2\right)\Phi(r,t) \;\;=\;\; 0\;\;. \tag{16}$$

As shown in Sec. 2.1, a general solution for *outgoing* waves is written as $\Phi(r-ct)$, such that for $l \geq 1$ the radial functions ψ_l are expressed as

$$\psi_l(r,t) \;\;=\;\; \prod_{i=1}^{l}\left(\partial_r \;-\; \frac{i-1}{r}\right)\frac{1}{r}\,\Phi_l(r\,-\,ct)\;\;. \tag{17}$$

Recursive use of this relations enables one after some rearrangement to rewrite the l-th radial function as a sum over l, i.e.

$$\begin{aligned}\psi_l(r,t) \;\;&=\;\; \sum_{i=0}^{l}\frac{(-)^i}{r^{i+1}}\,\rho_{l,i}\,\frac{\partial^{l-i}}{\partial r^{l-i}}\,\Phi_l(r\,-\,ct)\\ &=\;\; (-)^l\sum_{i=0}^{l}\frac{1}{c^{l-i}\,r^{i+1}}\,\rho_{l,i}\,\frac{\partial^{l-i}}{\partial t^{l-i}}\,\Phi_l(r\,-\,ct)\;\;,\end{aligned} \tag{18}$$

where $\rho_{l,i} = (l+i)!/[2^i\,i!\,(l-i)!]$. Note that in the last step we replaced the spatial derivative with a time derivative using

$$(-)^k\,\frac{\partial^k}{\partial r^k}\,\Phi_l(r\,-\,ct) \;\;=\;\; \frac{1}{c^k}\,\frac{\partial^k}{\partial t^k}\,\Phi_l(r\,-\,ct)\;\;. \tag{19}$$

In analogy with ref. [6] we replace the radial derivative with a time derivative by applying the operator B_1 on the radial function

$$B_1\,\psi_{lm} = \left(\partial_r \;+\; \frac{1}{c}\partial_t \;+\; \frac{1}{r}\right)\psi_{lm} = \frac{(-)^{l+1}}{r}\sum_{i=0}^{l}\frac{i\,\rho_{l,i}}{c^{l-i}\,r^{i+1}}\,\frac{\partial^{l-i}}{\partial t^{l-i}}\,\Phi_{lm}(r-ct) \tag{20}$$

Finally, using the multipole expansion (9) and multiplying the last expression by Y_{lm} where we sum over l and m, yields for $r = R$

$$B_1\,\psi(R,\vartheta,\varphi,t) \;=\; -\,\frac{1}{R}\sum_{l,m}Y_{lm}(\vartheta,\varphi)\sum_{i=1}^{l}\frac{(-)^l i\rho_{li}}{c^{l-i}R^{i+1}}\,\frac{\partial^{l-i}}{\partial t^{l-i}}\,\Phi_{lm}(R\,-\,ct)\,. \tag{21}$$

In the general case, the functions Φ_{lm} are obtained by evaluating Eq. (18) at $r = R$. Since $\rho_{l0} = 1$ this leads to the solution of a linear, differential equation of order l

$$\frac{1}{c^l}\frac{d^l}{dt^l}\,\tilde{\Phi}_{lm}(t) \;=\; -\sum_{i=1}^{l}\frac{\rho_{li}}{c^{l-i}R^i}\,\frac{d^{l-i}}{dt^{l-i}}\,\tilde{\Phi}_{lm}(R\,-\,ct)\;+\;\psi_{lm}(R,t) \qquad (22)$$

where we substituted $\tilde{\Phi}_{lm} = (-)^l\Phi_{lm}/R$ and the inhomogeneous term $\psi_{lm}(R,t)$ is given by Eq. (11) evaluated at $r = R$.

Expression (21) represents the exact nonreflecting boundary condition in the form obtained in [6] were an integral transforms formed the basis of the approach. Note that, in practical calculations, truncation of the summation over l at a finite value $l = L$ leads to an exact representation of modes with $l \le L$. Thus, the boundary condition reduces to $B_1\psi|_{r=R} = 0$ for harmonic modes with $l' > L$. In particular, $B_1\psi|_{r=R} = 0$ is an exact boundary condition for spherically symmetric modes ($l = 0$).

3 Numerical Results using Finite Differences

Using the results of the previous section, we illustrate the use of absorbing boundary conditions and their numerical implementation using a finite difference formulation. The wave equation is discretized both in space and time using centred finite differences. At time $t_k = k\,\Delta t$, we denote by $\Psi^k(n)$ the numerical approximation to the time dependent wave function $\psi(\mathbf{r},t)$ and by $f^k(n)$ the forcing term at the n-th grid point r_n in radial direction. The numerical solution is advanced in time using

$$\Psi^{k+1}(n) \;=\; 2\,\Psi^k(n) \;-\; \Psi^{k-1}(n) \;+\; (\Delta t)^2\,\left[\mathcal{D}\,\Psi^k(n) \,+\, f^k(n)\right] \quad , \qquad (23)$$

where $\mathcal{D}$ represents a finite difference approximation to the Laplace operator Δ. Using a second order finite difference approximation, the radial part $\mathcal{D}_r = (1/r^2)(r^2\partial_r)$ of the complete Laplacian $\mathcal{D}$ is expressed as

$$\mathcal{D}_r\Psi(n) \;=\; \frac{r^2_{n+1/2}\Psi(n+1) \,-\, (r^2_{n+1/2} + r^2_{n-1/2})\,\Psi(n) \,+\, r^2_{n-1/2}\Psi(n-1)}{(r_n\,\Delta r)^2} \quad , \qquad (24)$$

where $r_{n\pm1/2} = r_n \pm \Delta r/2$. Note from the above equation that the boundary condition is required when the Laplace operator is to be calculated at the outer most radial grid point r_n belonging to the boundary of the computational domain $\tilde{\Omega}$, i.e. at $r_n = R$. Inspection of the last expression clearly shows that this calculation uses values of $\Psi^k(n+1)$ belonging to the exterior region $\mathbb{R}^3 \setminus \tilde{\Omega}$.

However, one obtains an additional relation between the quantities $\Psi^{k+1}(n)$ and $\Psi^k(n+1)$ by using a finite difference representation of the boundary condition equation (21) at $r_n = R$. Consequently, the problem is solved by coupling the two equations for $\Psi^{k+1}(n)$ and $\Psi^k(n+1)$, allowing one to solve for $\Psi^{k+1}(n)$.

Note that the due to the local character of the absorbing boundary condition, only values at $t = t_k$ are needed in a given time step.

This procedure becomes particularly simple and is best illustrated using a cartesian grid $x_n = n\Delta x$ in one dimension. In this case Eq. (24) leads to the calculation of the second space derivative ∂_x^2

$$\mathcal{D}\,\Psi^k(n) \;=\; \frac{\Psi^k(n+1) \;-\; 2\,\Psi^k(n) \;+\Psi^k(n-1)}{(\Delta x)^2} \quad , \tag{25}$$

and the finite difference representation of the boundary condition reads

$$\frac{1}{c}\,\frac{\Psi^{k+1}(n) \;-\; \Psi^{k-1}(n)}{\Delta t} \quad + \quad \frac{\Psi^k(n+1) \;-\; \Psi^k(n-1)}{\Delta x} \quad = \quad 0 \quad , \tag{26}$$

where we used the one dimensional representation of the boundary condition (21) as given by eq. (7). The last expression may be rewritten as

$$\Psi^k(n+1) \quad = \quad -\,\frac{1}{c}\,\frac{\Delta x}{\Delta t}\,\left[\Psi^{k+1}(n) \;-\; \Psi^{k-1}(n)\right] \quad + \quad \Psi^k(n-1) \quad , \tag{27}$$

providing the additional equation for $\Psi^{k+1}(n)$. By combining these two equations for $\Psi^{k+1}(n)$ and $\Psi^k(n+1)$, one finds

$$\Psi^{k+1}(n) \quad = \quad \frac{2\,\Psi^k(n) \;+\; (\alpha-1)\Psi^{k-1}(n) \;+\; 2\,\alpha^2\,\left[\Psi^k(n-1) \;-\; \Psi^k(n)\right]}{1 \;+\; \alpha} \tag{28}$$

where $\alpha = c\Delta t/\Delta x$. This expression clearly shows that the evaluation of the time extrapolated function $\Psi^{k+1}(n)$ at the boundary does not depend on function values lying outside the computational domain.

Using the approach described above we are now in a position to analyse the time evolution of perturbations using absorbing boundary conditions. In Figures 1 and 2 we display snapshots of the wave function at different times for $t = 82, 128, 250, 450$, and 900, respectively. The contour plots on the right hand side of the figures display the position of time evolved waves in the $xy-$ plane, where the computational domain extends from an inner radius $r_< = 1000$ km to the outer radius $r_> = 6371$ km. Thus, the position of the artificial boundary at $R = r_>$ corresponds to the Earth's radius. The plots on the left show the dependence of the associated wave function on the radial coordinate r. While the starting point of the calculation is $t = 0$, the perturbing source is assumed to be proportional to a Gaussian $\exp(t - t_0)^2$ and is located at $r_0 \simeq 5000$ km. For $t = 82$ we observe a strong peak located in the vicinity of the source. In the contour plot on the right hand side, one sees that the wave is located in the area between the two bright circles.

For larger times, at $t = 128$, the wave separates in two independent contributions propagating in opposite directions along the radial coordinate r. While one of the waves moves outwards towards increasing r-values the other wave propagates inwards towards the rigid boundary associated with the inner circle, as indicated by the two arrows in the left figure. For later times, t = 250, it is seen that only

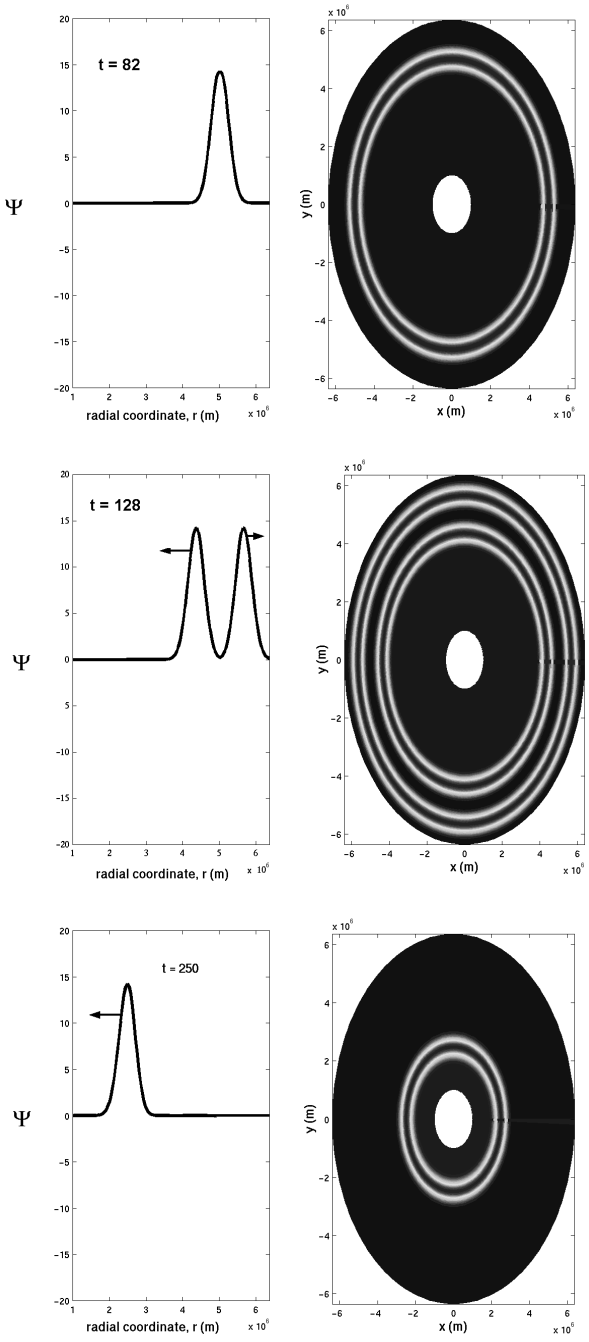

Fig. 1. Snapshots of the time evolved wave function obtained by the numerical solution of the wave function incorporating the nonreflecting boundary condition for $t = 82, 128,$ and $t = 250$. The initial wave separates in two parts propagating in opposite directions.

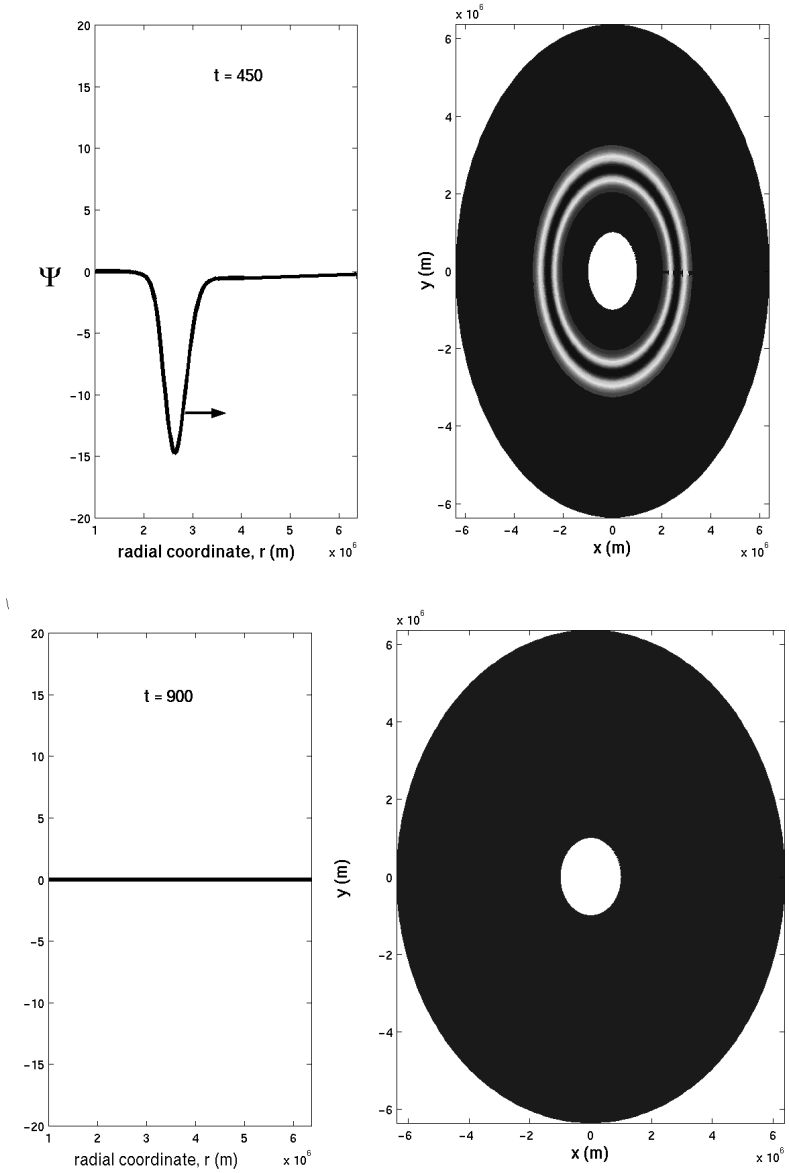

Fig. 2. The same as in Fig. 1 for larger times $t = 450$, and 900. At large asymptotic times both components leave the computational domain and no reflection at the artificial boundary is observed.

the ingoing wave can be found inside the computational region as the outgoing one passes the artificial boundary ar $r = R$ without any reflection. On the other hand, the ingoing wave propagating towards smaller r-values changes its sign and the direction of propagation after encountering the margin $r_<$ of the inner circle. As a result, for larger times ($t = 450$) this wave propagates towards the margin of the computational domain but with opposite sign. Finally, for even larger times this wave passes the artificial boundary at $r = R$ without any reflection. Thus, for $t = 900$ the computational region is seen to be completely unperturbed and, as a result of the absorbing boundary condition, the artificial boundary appears perfectly transparent to the wave as there is no spurious reflection.

4 Concluding Remarks

In conclusion, our numerical results are consistent with and complement the analytic representation of the nonreflecting boundary condition discussed in Sec. 2. As there is no unphysical reflection at the artificial boundary associated with the computational region this condition ensures perfect transparency. It is important to note that since the derivation of the boundary condition depends only on the behaviour in the exterior domain, the problem inside the computational region can be arbitrarily complex. As a main result, numerical schemes for wave propagation incorporating nonreflecting boundary conditions are shown to display a very long time stability.

Acknowledgement

This work was supported in part by the University of Queensland under Grant No. UQRSF 2002001336, by the Australian Research Council and by the International Quality Network (IQN) Georisk Program at the University of München.

References

1. Tsynkov, S.V.: Appl. Num. Math. **27**, 465 (1998).
2. Clayton, R.W. and Engquist, B.: Bull. Sei. Soc. Am. **67**, 1529 (1977).
3. Engquist, B. and Majda, A.: Commun. Pure Appl. Math. **32**, 313 (1979).
4. Higdon, R.L.: SIAM J. Num. Anal. **27**, 831 (1990).
5. Israeli, M. and Orszag, S.A.: J. Comput. Phys. **41**, 115 (1981).
6. Grote, M.J. and Keller, J.B.: SIAM J. Appl. Math. **55**, 280 (1995); and **60**, 803 (2000).
7. Grote, M.J. and Keller, J.B.: J. Comput. Phys. **139**, 327 (1998).
8. Ionescu, D.C. and Belkacem, A.: Phys. Scripta **T80**, 128 (1999).
9. Ionescu, D.C. and Belkacem, A.: Eur. Phys. Journal D **18**, 301 (2002).
10. Thompson L. and Huan R.: to appear in Comp. Meth. Appl. Mech. Eng (2003).
11. Lamb, H.: *Hydrodynamics*. (Cambridge University Press, 1916).